Comparative Verification of Radiation Noise Reduction Effect using Spread Spectrum for Inductive Power Transfer System

Keisuke Kusaka [1)] Kent Inoue [2)] Jun-ichi Itoh [3)]

1)Nagaoka Univesity of Technology, Dept. of Electrical, Electronics and Information

1603-1 Kamitomioka-machi, Nagaoka, Niigata, 940-2188, Japan (E-mail: kusaka@vos.nagaokaut.ac.jp)

2) Nagaoka University of Technology, Dept. of Electrical, Electronics and Information

1603-1 Kamitomioka-machi, Nagaoka, Niigata, 940-2188, Japan (E-mail: k_inoue@stn.nagaokaut.ac.jp)

3) Nagaoka University of Technology, Dept. of Electrical, Electronics and Information

1603-1 Kamitomioka-machi, Nagaoka, Niigata, 940-2188, Japan (E-mail: itoh@vos.nagaokaut.ac.jp)

Presented at EVS 31 & EVTeC 2018, Kobe, Japan, October 1 - 3, 2018

ABSTRACT: This paper evaluated radiation noise reduction methods for inductive power transfer systems using a spread spectrum technique. In the spread spectrum methods, the radiation noise is reduced by changing a switching frequency, which is generated by pseudorandom numbers at random, continuously. The effects of the radiation noise reduction are evaluated with the IPT system with a series-parallel compensation and series-series compensation topology. As the results, the harmonics components of the radiation noise around the fundamental frequency are reduced by 7.8 and 8.1 dBμA in maximum with the series-series compensation method and the series-parallel compensation method, respectively in comparison with the constant frequency transmission. From the results, the proposed methods are effective for both the series-series compensation and series-parallel compensation method.

KEY WORDS: Inductive power transfer, Radiation noise, Spread spectrum, Series-series (SS) compensation, Series-parallel (SP) compensation

1. INTRODUCTION

In recent years, inductive power transfer (IPT) systems for electric vehicles (EVs) have been actively studied and developed [1-7]. In particular, practical realization of the IPT systems for EVs or plug-in hybrid EVs (PHEVs) is highly desired because the IPT systems are capable of improving the usability of the EVs and the PHEVs. However, the IPT systems emit radiation noise. Therefore, in order to employ the IPT systems into practical applications, the radiation noise must be suppressed to satisfy existing standards, such as the well-known standard based on CISPR11, i.e., a standard regulated by the International special committee in radio interference. Otherwise, the IPT systems might affect other wireless communication systems or electronic equipment.

Figure 1 shows the maximum allowable radiation noise for the IPT systems of 7 kW or less for EVs in Japan. In Japan, the allowable radiation noise has been legislated. The regulations are currently under discussion for the international standardization. A 85-kHz frequency band will be used as the transmission frequency in the international standard. This regulation is basically corresponding to CISPR 11 Group 2, Class B [8].

In previous studies, suppression methods using a magnetic material or metal shield have been proposed [9-12]. In order to suppress the radiation noise, transmission coils are surrounded by plates composed of a magnetic material or metal plate. The radiation noise can be suppressed because these shields convert the magnetic flux from the radiation noise into eddy currents. However, the eddy currents increase the power loss of the IPT systems. Moreover, the additional shields (magnetic or metal) lead to an increase in cost. So far, the authors have proposed two radiation noise reduction methods, in which the power is transmitted with changing switching frequency of the inverter continuously; it is also called as a spread spectrum [13-14]. The proposed methods do not need additional components. Moreover,

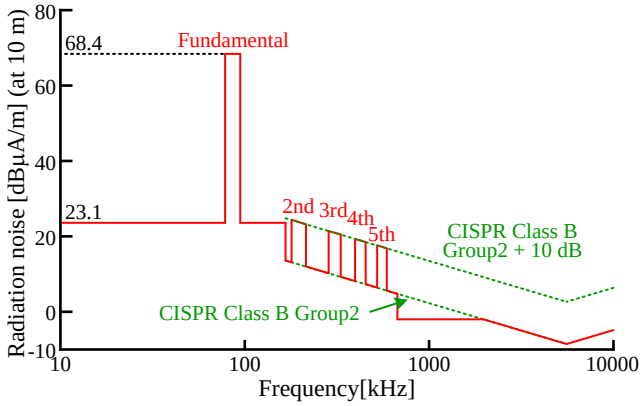

Fundamental	79 kHz – 90 kHz
2nd	158 kHz – 180 kHz
3rd	237 kHz – 270 kHz
4th	316 kHz – 360 kHz
5th	395 kHz – 450 kHz

Fig. 1. Maximum allowable radiation noise for IPT system of 7 kW or less for use in EVs in Japan (under discussion).

the effect on the efficiency by using the proposed method is small at the rated power [14]. In a previous paper, the radiation noise reduction effect of these two proposed methods have been evaluated with the IPT system with a series-series (SS) compensation topology. However, the effectiveness of the proposed radiation noise reduction methods for the IPT system with a series-parallel (SP) compensation topology had not been evaluated.

In this paper, the proposed radiation noise reduction technique is used for the IPT system with the SP compensation topology . The contribution of this paper is that the radiation noise reduction effect is compared between the SS and the SP compensation topology.

2. RADIATION NOISE REDUCTION METHODS

2.1. Generation method of pseudorandom number

In the proposed method, the radiation noise is spread over the frequency domain from 80 kHz to 90 kHz by changing the switching frequency of the inverter in two different ways. The switching frequency is changed according to pseudorandom numbers, which are generated by using a maximum length sequence (M-sequence). The M-sequence random number is generated as

$$X_z = X_{z-p} \oplus X_{z-q} \quad \text{.....(1)},$$

where X_{z-p} and X_{z-q} are the present values of X_z delayed by periods of p and q, respectively ($p > q$). In this paper, $p = 7$ and $q = 1$ are used. Note that a number of bits of the pseudorandom number is seven.

2.2. Probability distributions for reduction method

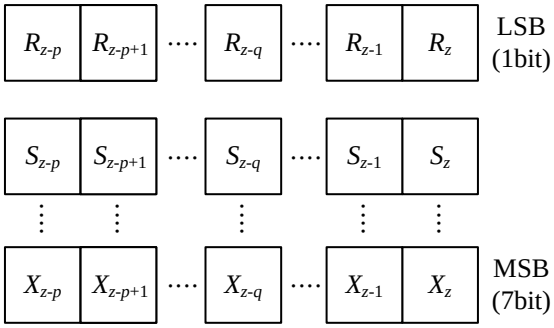

Fig. 2. Generation method of pseudorandom numbers based on maximal length sequence.

Figure 3 shows the probability distribution of the switching frequency of the inverter in two proposed radiation noise reduction methods. Fig. 3 (a) shows the probability distribution of spread spectrum with a uniform distribution (SSUD) [2]. The probability distribution is a discrete uniform distribution from 80 kHz to 90 kHz. Therefore, the spectrum of the voltage applying to the transmission coil is uniformly spread. Fig. 3 (b) shows the probability distribution of spread spectrum with a biased distribution (SSBD) [3]. The input impedance depends on the switching frequency. Thus, the probability distribution is in proportional to the impedance of resonance circuit.

3. DESIGN OF TRANSMISSION COIL

Figure 4 shows the equivalent circuit for designing the IPT system. Fig. 4 (a) and (b) show the SS compensation topology and the SP compensation topology, respectively.

3.1. SS compensation method

From the circuit equations of the equivalent circuit, which is shown in Fig. 4 (a), the primary current and the secondary current are calculated as

$$\dot{I}_1 = \frac{r_2 + R_{eq} + j\left(\omega L_2 - \frac{1}{\omega C_2}\right)}{\left\{r_1 + j\left(\omega L_1 - \frac{1}{\omega C_1}\right)\right\}\left\{r_2 + R_{eq} + j\left(\omega L_2 - \frac{1}{\omega C_2}\right)\right\} + \omega^2 L_m^2}\dot{V}_1 \quad \text{.....(2),}$$

$$\dot{I}_2 = \frac{j\omega L_m}{\left\{r_1 + j\left(\omega L_1 - \frac{1}{\omega C_1}\right)\right\}\left\{r_2 + R_{eq} + j\left(\omega L_2 - \frac{1}{\omega C_2}\right)\right\} + \omega^2 L_m^2}\dot{V}_1 \quad \text{.....(3),}$$

where V_1 is the primary voltage, R_{eq} is the equivalent load resistance, r_1 is the equivalent series resistance of the primary winding, r_2 is the equivalent series resistance of the secondary winding, L_1 is the primary inductance, L_2 is the secondary inductance, C_1 is the primary compensation capacitor, C_2 is the secondary compensation capacitor, L_m is the mutual inductance, and ω is the angular frequency of the power supply. Note that the voltage V_1 is the fundamental component of the output voltage of the inverter.

The parameters of the transmission coil are designed with the equivalent circuit. The resistance R_{eq} indicates that equivalent load resistance considering the full-bridge rectifier. Then the equivalent load resistance is given by [15]

$$R_{eq} = \frac{8}{\pi^2}\frac{V_{DC,2}^2}{P_2} \quad \text{.....(4),}$$

where $V_{DC,2}$ is the DC voltage on the secondary side and P_2 is the output power.

The inductances of the primary and the secondary coils are designed according to the following equations

$$L_1 = \frac{R_{eq}}{\omega k}\frac{V_{DC,1}^2}{V_{DC,2}^2} \quad \text{.....(5),}$$

$$L_2 = \frac{R_{eq}}{\omega k} \quad \text{.....(6),}$$

where $V_{DC,1}$ is the DC voltage on the primary side and k is the coupling coefficient.

The compensation capacitors are selected in order to cancel out the reactive power at the input frequency. Thus, the value of the compensation capacitors is calculated as

$$C_1 = \frac{1}{\omega^2 L_1} \quad \text{.....(7),}$$

$$C_2 = \frac{1}{\omega^2 L_2} \quad \text{.....(8).}$$

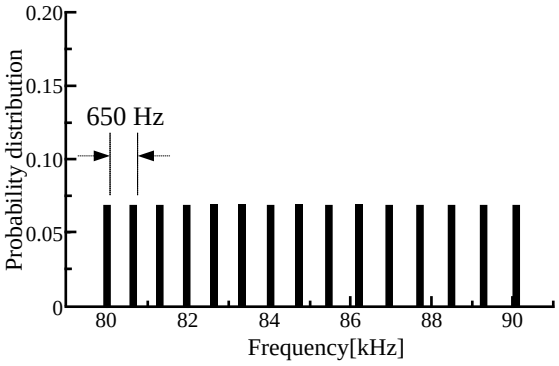

(a) Proposed method I: SSUD

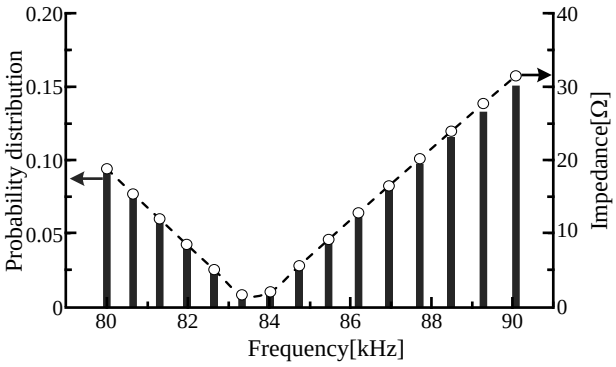

(b) Proposed method II: SSBD

Fig. 3. Probability distributions for proposed methods. Changing range of switching frequency of inverter is from 80 kHz to 90 kHz.

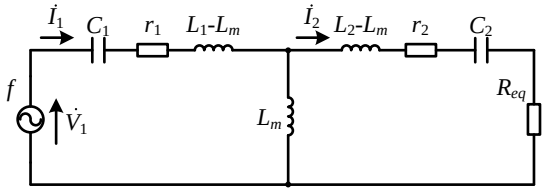

(a) SS compensation method.

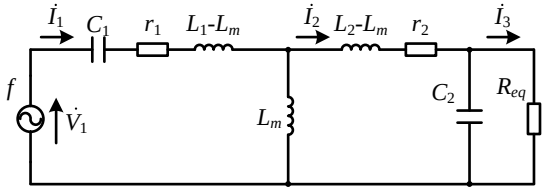

(b) SP compensation method.

Fig. 4. Equivalent circuit for designing the IPT system.

3.2. SP compensation method

The circuit equations of the equivalent circuit, which is shown Fig. 4 (b) are calculated as

$$\dot{I}_1 = \frac{\left\{ r_2 + j\left(\omega L_1 - \frac{1}{\omega C_2} \right) \right\} \left(R_{eq} - j\frac{1}{\omega C_2} \right) + \frac{1}{\omega^2 C_2^2}}{\Delta} \dot{V}_1 \quad \text{....(9),}$$

$$\dot{I}_2 = \frac{j\omega L_m \left(R_{eq} - j\frac{1}{\omega C_2} \right)}{\Delta} \dot{V}_1 \quad \text{.....(10),}$$

$$\dot{I}_3 = \frac{1}{\Delta} \frac{L_m}{C_2} \dot{V}_1 \quad \text{.....(11),}$$

$$\Delta = \begin{vmatrix} r_1 + j\omega\left(L_1 - \frac{1}{\omega^2 C_1} \right) & -j\omega L_m & 0 \\ -j\omega L_m & r_2 + j\omega\left(L_2 - \frac{1}{\omega^2 C_2} \right) & j\frac{1}{\omega C_2} \\ 0 & j\frac{1}{\omega C_2} & R_{eq} - j\frac{1}{\omega C_2} \end{vmatrix}$$

.....(12).

Note that the voltage $\boldsymbol{V}_1$ is the fundamental component of the output voltage of the inverter.

The parameters of the transmission coil are designed with the equivalent circuit. The resistance R_{eq} indicates the equivalent load resistance considering the full-bridge rectifier. Then the equivalent load resistance is given by [15]

$$R_{eq} = \frac{\pi^2}{8} \frac{V_{DC,2}^2}{P_2} \quad \text{.....(13).}$$

The inductances of the primary and the secondary coils are designed according to the following equations

$$L_1 = L_2 \left(\frac{8}{\pi^2 k} \frac{V_{DC,1}}{V_{DC,2}} \right)^2 \quad \text{.....(14),}$$

$$L_2 = \frac{R_{eq}}{\omega} \frac{k}{\sqrt{1+k^2}} \quad \text{.....(15),}$$

The compensation capacitors are selected in order to cancel out the reactive power at the input frequency. Thus, the value of the compensation capacitors is calculated as

$$C_1 = \frac{1}{\omega^2 L_1 \left(1 - k^2 \right)} \quad \text{.....(16),}$$

$$C_2 = \frac{1}{\omega^2 L_2} \quad \text{.....(17).}$$

4. EXPERIMENTAL RESULTS

4.1. Experimental Setup

Figure 5 and Table I show the circuit configurations for the prototype and specifications, respectively. The self-inductance of the primary side and secondary side in Table I is measured from the prototype of the transmission coils. The silicon carbide

Table I. Specifications of prototype.

	Symbol	Value
Input DC voltage	V_{in}	420 V
Rated power	P	3.0 kW
Coupling coefficient	k	0.20
Primary inductance	L_1	392 μH
Secondary inductance	L_2	401 μH (SS) 24.2 μH (SP)
Primary capacitance	C_1	8.96 nF
Secondary capacitance	C_2	8.78 nF (SS) 145 nF (SP)
Transmission distance	l	150 mm

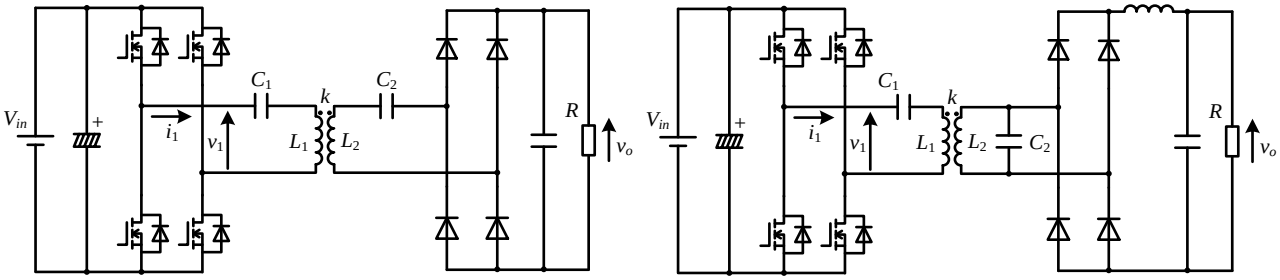

(a) SS compensation method. (b) SP compensastion method.

Fig. 5. Circuit configrations of prototype.

MOSFETs are used as the switching devices in the inverter. Also, the silicon carbide schottky barrier diodes are used in the rectifier.

Figure 6 shows the primary and secondary coils for the prototype. The common solenoid-type coils are used for the both compensation topology. In order to obtain the common output power, the number of turns of the secondary coil is different between the SS compensation and SP compensation topology. The transmission distance is 150 mm, assuming transmission from the road to the bottom of the EV or PHEV.

4.2. Radiation Noise Measurement Conditions

Figure 7 shows the setup of the probe used for the measurement of the radiation noise. The radiation noise was measured at two points. The each distance from the edge of the transmission coils and to each measurement position is 500 mm.

4.3. Experimental Results

Figure 8 shows the radiation noise with the SS compensation method. Fig. 8 (a) shows the result with a constant switching frequency operation, whereas Fig. 8 (b) and (c) show the results using the spread spectrum with SSUD and SSBD, respectively. As a result, by using the SSUD and SSBD, the radiation noise on the fundamental frequency is reduced by 4.8 dBμA and 7.8 dBμA in comparison with the conventional method. In addition, the effect of reduction is confirmed at low-order harmonics components, similarly.

Figure 9 shows the radiation noise with the SP compensation method. Fig. 9 (a) shows the result with a constant switching frequency operation, whereas Fig. 9 (b) and (c) show the results obtained using the SSUD and SSBD, respectively. As a result, by using the SSUD and SSBD, the fundamental frequency is reduced by 4.8 dBμA and 8.1 dBμA in comparison with the conventional method. In addition, the effect of reduction is confirmed at low-order harmonics components, similarly. As a result, the proposed radiation noise reduction methods are effective for both the SP and SS topology. The reduction effect of the radiation noise is almost equivalent.

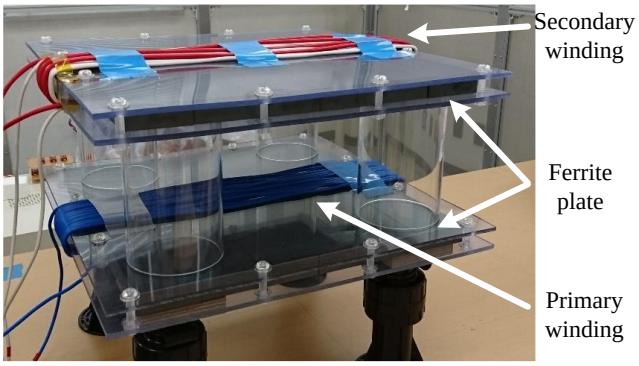

Fig. 6. Transmission coils with rated power of 3 kW. Lower side is transmitter coil, upper side is receiver coil. White winding in secondary side is used SS compensation method. Red winding in secondary side is used SP compensation method.

5. CONCLUSION

So far, the authors have proposed two radiation noise reduction methods, in which the power is transmitted by a continuously changing switching frequency of the inverter over a spread spectrum.

In this paper, the radiation noise reduction effect of two proposed methods (the SSUD and the SSBD) was experimentally demonstrated with the IPT system of 3 kW prototype employing SP compensation method. In addition, the reduction effect was evaluated in comparison with employing the SS compensation method. As a result, the harmonics components around the

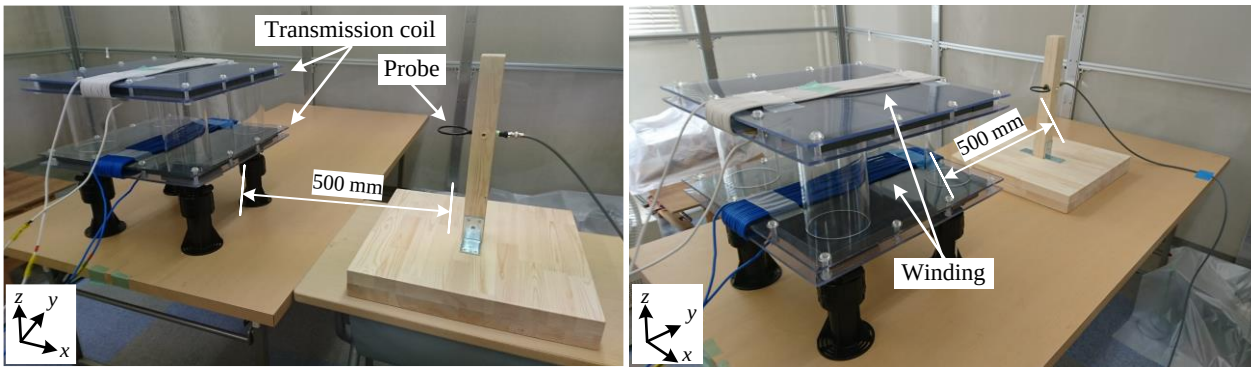

(a) Measurement point: A. (b) Measurement point: B.

Fig. 7. Measurement environment of radiation noise. The distance from edge of transmission coils to each measurement position is 500 mm.

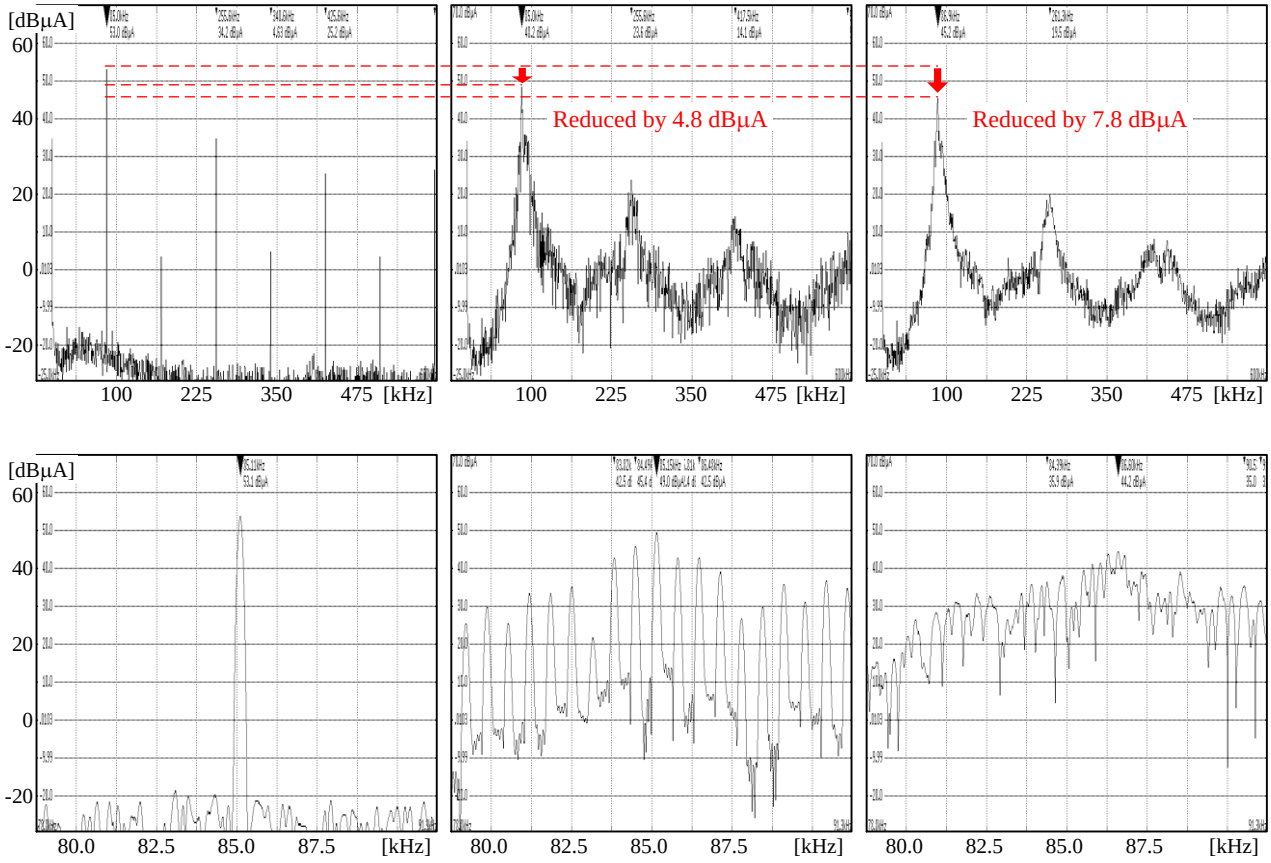

(a) Conventional method. (b) Proposed method I: SSUD. (c) Proposed method II: SSBD.

Fig. 8. Radiation noise at measurement point A in y-z plane with SS compensation topology.

fundamental frequency of the radiation noise with the SS compensation method were suppressed by 4.8 and 7.8 dBμA by applying the SSUD and the SSBD, respectively. On the other hand, in the SP compensation method, the harmonics components around the fundamental frequency of the radiation noise were suppressed by 4.8 and 8.1 dBμA by applying the SSUD and the SSBD, respectively. From the results, the radiation noise reduction effect is expected using the two proposed methods the IPT system employing the SP compensation method as with the SS compensation method.

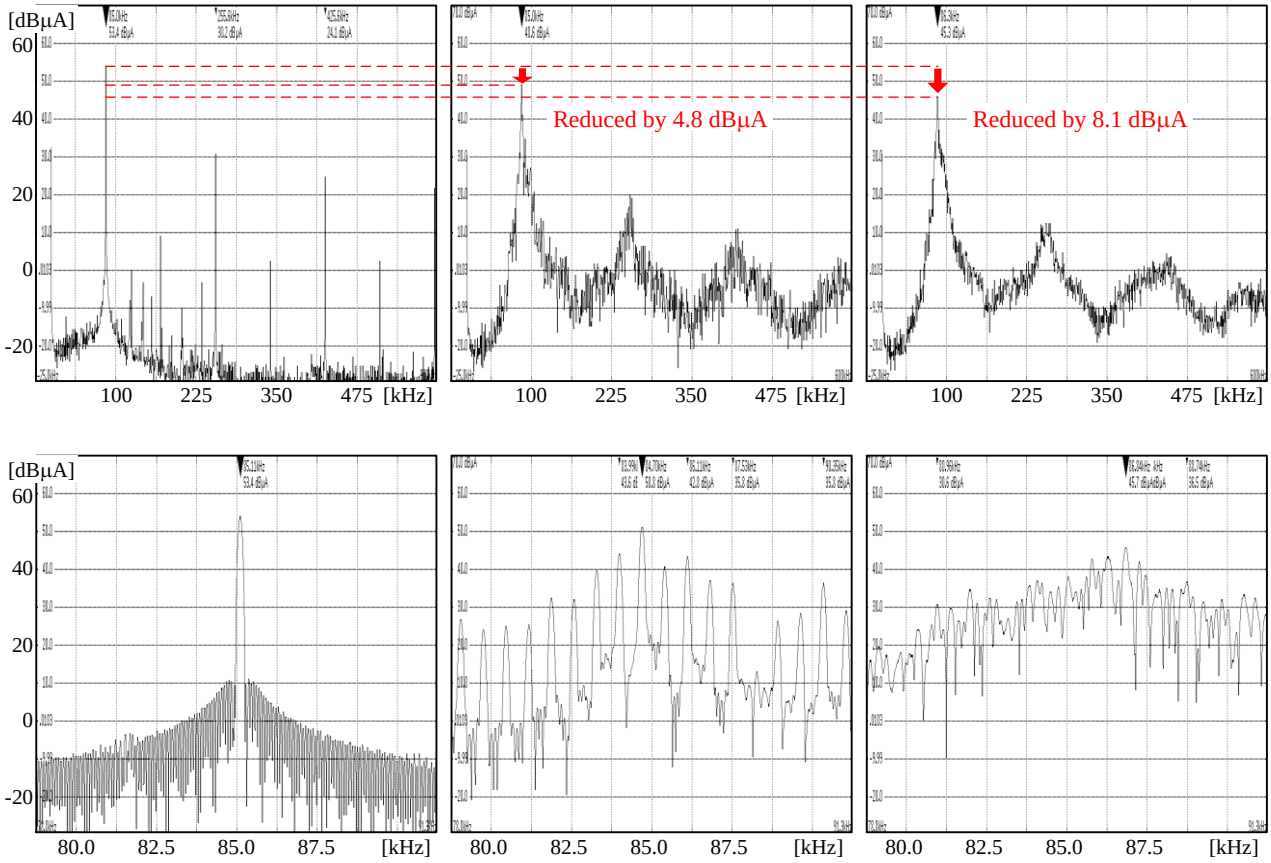

(a) Conventional method. (b) Proposed method I: SSUD. (c) Proposed method II: SSBD.

Fig. 9. Radiation noise at measurement point A in y-z plane with SP compensation method.

REFERENCES

[1] S. Y. R. Hui, W. Zhong, C. K. Lee: "A Critical Review of Recent Progress in Mid-Range Wireless Power Transfer," IEEE Trans. Power Electron., vol. 29, no. 9, pp. 4500-4511, Sep. 2014.

[2] D. Shimode, T. Mura, S. Fujiwara, "A Study of Structure of Inductive Power Transfer Coil for Railway Vehicles," IEEJ J. Ind. Appl., vol. 4, no. 5, pp. 550-558, Sep. 2015

[3] Y. Hayashi, Y. Chiku, "Contactless DC Connector Concept for High-Power –Density 380-V DC Distribution System," IEEJ J. Ind. Appl., vol. 4, no. 1, pp. 49-58, Jan. 2015.

[4] K. Kusaka, K.Orikawa, J. Itoh, I. Hasegawa, K. Morita, T. Kondo, "Galvanic Isolation System with Wireless Power Transfer for Multiple Gate Driver Supplies of a Medium-voltage Inverter," IEEJ J. Ind. Appl., vol. 5, no. 3, pp. 206-214, May. 2016.

[5] T. Mizuno, T. Ueda, S. Yashi, R. Ohtomo, Y. Goto, "Dependence of Efficiency on Wire Type and Number of strands of Litz Wire for Wireless Power Transfer of Magnetic Resonant Coupling," IEEJ J. Ind. Appl., vol. 3, no. 1, pp. 35-40, Jan. 2014.

[6] N. K. Trung, T. Ogata, S. Tanaka, K. Akatsu, "Analysis and PCB Design of Class D Inverter for Wireless Power Transfer Systems Operating a 13.5 MHz," IEEJ J. Ind. Appl., vol. 4, no. 6, pp. 703-713, Nov. 2015.

[7] J. T. Boys, G. A. Covic, Y. Xu: "DC Analysis Technique for Inductive Power Transfer Pick-Ups," IEEE Trans. Power Electron., vol. 1, no. 2, pp. 51-53, Jun. 2003.

[8] Ministry of Internal Affairs and Communications, Japan, "Inquiry of technical requirements for wireless power transfer system for EVs in technical requirements for wireless power transfer system in standards of International Special Committee on Radio Interference (CISPR)," 2015.

[9] M. Jo, Y. Sato, Y. Kaneko, S. Abe: "Methods for Reducing Leakage Electric Field of a Wireless Power Transfer System for Electric Vehicles", IEEE Energy Conversion Congress Expo, pp.1762-1769, (2014)

[10] H. Kim, J. Cho, S. Ahn, J. Kim, J. Kim: "Suppression of Leakage Magnetic Field from a Wireless Power Transfer System using Ferrimagnetic Material and Metallic Shielding," IEEE Int. Symp. Electromagnetic Compatibility, pp. 640-645, Aug. 2012.

[11] T. Campi, S. Cruciani, M. Feliziani: "Magnetic Shielding of Wireless Power Transfer Systems," IEEE Int. Symp. Electromagnetic Compatibility, pp. 422-425, May 2014.

[12] K. Maikawa, K. Imai, Y. Minagawa, M. Arimitsu, H. Iwao: "Magnetic Field Reduction Technology of Wireless Charging System," JSAE Congr. Autumn, no. 110-13, Oct. 2013.

[13] K. Kusaka, K. Inoue, J. Itoh: "Reduction in Radiation Noise Level for Inductive Power Transfer System with Spread Spectrum", The International Electric Vehicle Technology & Automotive Power Electronics Japan Conference, No. 20169063 (2016)

[14] K. Inoue, K. Kusaka, J. Itoh: "Reduction in Radiation Noise Level for Inductive Power Transfer Systems using Spread Spectrum Techniques", IEEE Transaction on Power Electronics, Vol. 33, No. 4, pp. 3076-3085, (2018)

[15] R. Bosshard, J. W. Kolar, J. Muhlethaler, I. Stevanovic, B. Wunsch, F. Canales: "Modeling and η-α-Pareto Optimization of Inductive Power Transfer Coils for Electric Vehicles," IEEE J., vol. 3, no. 1, pp. 50-64, Mar. 2014.